



## Communication

# Palladium nanoflowers supported on amino-fullerene as novel catalyst for reduction of 4-nitrophenol



Zhongping Li\*, Chunxiao Han

Institute of Environmental Science, Shanxi University, Taiyuan 030006, China

## ARTICLE INFO

## Article history:

Received 7 June 2019

Received in revised form 24 June 2019

Accepted 25 June 2019

Available online 25 June 2019

## Keywords:

Palladium nanoflowers

Self-assembly

4-Nitrophenol

Amino-functionalized fullerene

Catalyst

## ABSTRACT

In this study, we report the synthesis of novel palladium nanoflowers (Pd NFs) on amino-functionalized fullerene ( $C_{60}$ -NH<sub>2</sub>) by hydrothermal self-assembly growth using ethylenediamine (EA) as a functional reagent. The successful formation of Pd nanoflowers supported amino-functionalized fullerene ( $C_{60}$ -NH<sub>2</sub>/Pd NFs) is evidenced by UV-vis and powder X-ray diffraction (XRD). The morphology of Pd NFs over the  $C_{60}$ -NH<sub>2</sub> surface has been investigated by high-resolution transmission electron microscopy (TEM) and Fourier-transform infrared (FT-IR) techniques. The supported Pd nanoflowers (Pd NFs/ $C_{60}$ -NH<sub>2</sub>) exhibit remarkably superior catalytic activity toward the reduction of 4-nitrophenol (4-NP). It exhibits remarkable UV-vis spectra response from 4-nitrophenol to 4-aminophenol (4-AP) (99% in 2.0 min) with a turnover frequency of 12.35 min<sup>-1</sup>. Its excellent catalytic stability and durability offer the promising application in catalysis.

© 2019 Chinese Chemical Society and Institute of Materia Medica, Chinese Academy of Medical Sciences. Published by Elsevier B.V. All rights reserved.

4-Nitrophenol (4-NP) is among the mostly used chemicals in the industry [1,2]. However, the elimination of 4-NP from water waste is an important issue in environmental science because 4-NP is a general organic pollutant generated during industrial or agricultural processes. Various methods have been applied to eliminate 4-NP, mainly includes: adsorption, photocatalysis, advanced oxidation processes, catalytic chemical oxidation, and nitro group reduction [3–7]. Among these methods, the reduction has been commonly adopted for the obvious advantages of mild reaction conditions, simple reaction treatment, and environmental friendliness. Moreover, its reduction product (aminophenol) can be reused. Therefore, it is virtually significant to develop effective catalysts for the reduction of 4-NP.

Due to their unprecedented activities, noble metal nanoparticles have attracted significant interest in catalysis science and engineering. Palladium nanoparticles (Pd NPs) catalysts are now obtaining attention because of their unique catalytic activity in the treatment of wastewater containing 4-NP [8]. Moreover, shape-controlled palladium nanomaterials have important application value in the field of catalysis. Moreover, ligands play a key role in the preparation of nanomaterials with different morphologies [9]. Herein, Pd nanoflowers (Pd NFs) was firstly developed using amino-functionalized fullerene ( $C_{60}$ -NH<sub>2</sub>) as a supporting platform

by a facile self-assembly hydrothermal approach (referred to as Pd NFs/ $C_{60}$ -NH<sub>2</sub>). Assembly growth prepared Pd NFs/ $C_{60}$ -NH<sub>2</sub> exhibited further improvement of catalytic activity and stability for the reduction of 4-nitrophenol (4-NP) to 4-aminophenol (4-AP) by UV-vis spectra. We believe that fullerene nano-platforms supported novel metal nanoflowers will offer promising applications in catalysis.

Amine functionalized fullerene ( $C_{60}$ -NH<sub>2</sub>) was synthesized according to the procedure of previous study [10]. The resulting dark brown solid products ( $C_{60}$ -NH<sub>2</sub>) were dried in vacuum at 60 °C for 24 h. Pd nanoflowers were synthesized as follows. Palladium chloride precursor (PdCl<sub>2</sub> ≥ 99.9%) in the amount of 0.02 mmol was dissolved in two drops of HCl (36.5%), then added into a mixture of 40 mL *N,N*-dimethylformamide (DMF) of with 1 mg  $C_{60}$ -NH<sub>2</sub> (the mass rate of Pd:  $C_{60}$ -NH<sub>2</sub> is 1:2) together. The combination was then placed into a Teflon<sup>®</sup>-lined autoclave. The autoclave was purged with N<sub>2</sub> for three times. After that, heated and conditioned at 140 °C for 6 h without stirring, followed by separating and washing with ethanol, vacuum drying at 60 °C overnight. The yield of Pd NF/ $C_{60}$ -NH<sub>2</sub> was ca. 90%. The catalytic activity of different Pd nanocomposites was tested by the reduction of 4-nitrophenol (4-NP) to 4-aminophenol (4-AP) using NaBH<sub>4</sub> as the reducing agent. In a typical test, 4-NP (2.3 mmol/L) was first mixed with fresh NaBH<sub>4</sub> (0.032 mol/L) aqueous solution (the molar ratio of NaBH<sub>4</sub> to 4-NP was 200:1) from which 1 mL of the mixture solution was transferred to the quartz cuvette. A 10 μL portion of catalyst Pd NFs/ $C_{60}$ -NH<sub>2</sub> (1 mg/mL) was introduced into the cuvette followed

\* Corresponding author.

E-mail address: [z1104@sxu.edu.cn](mailto:z1104@sxu.edu.cn) (Z. Li).

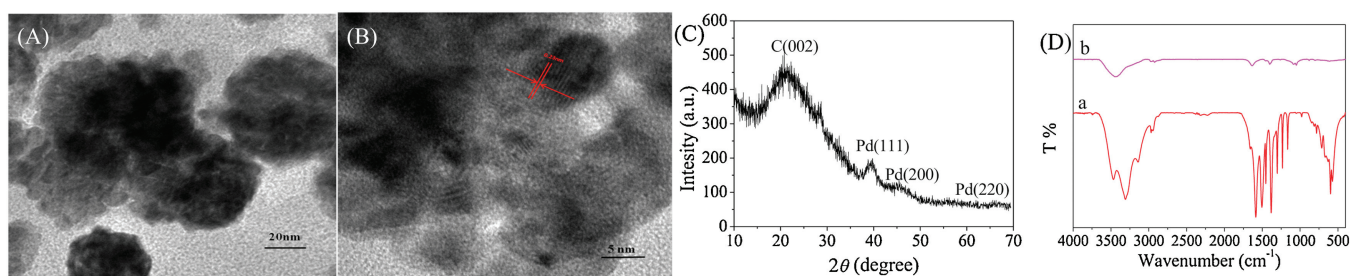


Fig. 1. (A) TEM image, (B) HRTEM image and (C) XRD patterns of Pd NFs/C<sub>60</sub>-NH<sub>2</sub> nanocomposites. (D) The FT-IR spectra of C<sub>60</sub>-NH<sub>2</sub> (a) and (b).

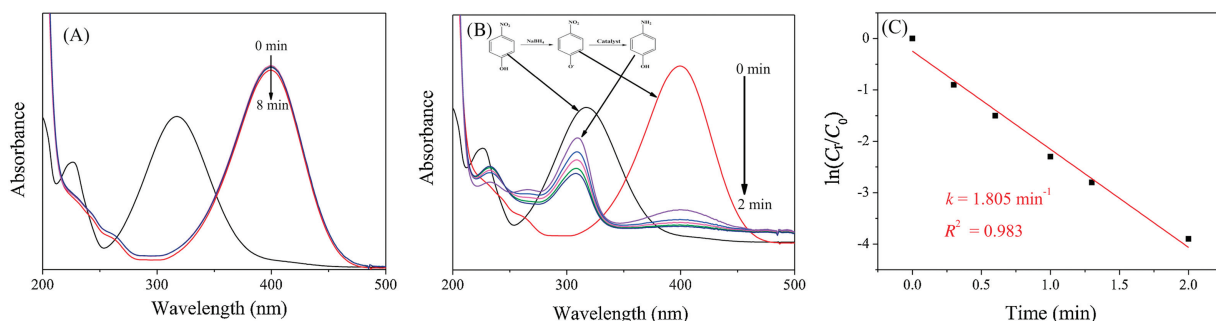


Fig. 2. The time-dependent UV-vis of 4-NP reduction with NaBH<sub>4</sub> in the absence (A) and presence (B) of the catalysts Pd NFs/C<sub>60</sub>-NH<sub>2</sub>. The plot of  $\ln(C_t/C_0)$  versus reaction time for the 4-NP reduction by catalysts (C).

Table 1

Comparison of catalytic performance for 4-NP with Pd NFs/C<sub>60</sub>-NH<sub>2</sub> and other catalysts reported.

Catalysts	Mass of catalysts (mg)	Amount of 4-NP (mmol)	Metal content (wt%)	Conversion time (min)	TOF value (min <sup>-1</sup> )	References
Pd@ASNTs	2	$6.0 \times 10^{-2}$	1.52	0.67	313.5	[13]
Pd@NC	0.025	$1.0 \times 10^{-4}$	2	6.5	3.27	[14]
PdCo@HCS-800	0.025	$1.73 \times 10^{-3}$	8.9	13.5	6.16	[15]
Pd-ZnO	5	$3.0 \times 10^{-4}$	0.05	1.5	8.64	[16]
Pd-rGO-CNT	5	$3.0 \times 10^{-4}$	1.12	0.33	1.71	[17]
Pd NFs/C <sub>60</sub> -NH <sub>2</sub>	0.01	$1.15 \times 10^{-3}$	4.95	2	12.35	This work

by rapid mixing with the pipetting over 2 s. The reaction kinetics at room temperature was monitored at different time by UV-vis scans between 200 nm and 500 nm. The maximum absorption was recorded at 400 nm and used for evaluating the concentration of 4-NP.

To increase the effective anchoring sites, ethylenediamine (EA) rich of amino-group (-NH<sub>2</sub>) is introduced to the surface of C<sub>60</sub> by the intrinsic strong electron deficient olefins properties of C<sub>60</sub>. The Pd NFs/C<sub>60</sub>-NH<sub>2</sub> nanoflowers were assembled successfully without stirring. The representative transmission electron microscopic (TEM) image of Pd NFs/C<sub>60</sub>-NH<sub>2</sub> (Fig. 1A) demonstrated coating densely of Pd NFs on the C<sub>60</sub>-NH<sub>2</sub> surface. Fig. 1B shows high-resolution TEM (HRTEM) image of the Pd NFs/C<sub>60</sub>-NH<sub>2</sub>, which revealed Pd nanoflower on the surface of C<sub>60</sub> sheet. X-ray diffraction (XRD) spectra of Pd NFs/C<sub>60</sub>-NH<sub>2</sub> was shown in Fig. 1C. XRD revealed (002) planes of C<sub>60</sub> peak at 20.0°. However, the weak peaks at 40.0, 46.7, and 68.3°, were assigned to the (111), (200) and (220) planes, respectively, of Pd from the *Fm3m* space group of the face-centered cubic (fcc) structure [11]. It additionally confirmed the presence of Pd nanoparticles in the nanocomposite of Pd NFs/C<sub>60</sub>-NH<sub>2</sub>, but the crystal structure of palladium nanoparticles is not obvious. Additionally, comparing with the FT-IR spectra of C<sub>60</sub>-NH<sub>2</sub>, the characteristic band -NH of Pd NFs/C<sub>60</sub>-NH<sub>2</sub> is significantly smaller at 3440 cm<sup>-1</sup> corresponding to N-H stretching and the band of N-H bending at 1630 and 915 cm<sup>-1</sup>,

which demonstrate the covalent attachment of amine to the surface of C<sub>60</sub> (Fig. 1D).

The catalytic performances of Pd NFs/C<sub>60</sub>-NH<sub>2</sub> were first evaluated through the reduction reaction of 4-nitrophenol (NP) to 4-aminophenol (AP) in the presence of NaBH<sub>4</sub>. Because both the 4-NP and the 4-AP have characteristic UV-vis absorption, it is readily easy to monitor the progress of the reaction by an UV-vis spectrophotometer. Without a catalyst, the reduction reaction, however, cannot proceed (Fig. 2A). The UV-vis absorption peak of 4-nitrophenol (4-NP) appears at  $\lambda_{\max} = 316$  nm. 4-Nitrophenolate ion was formed after the addition of NaBH<sub>4</sub>, which could be found by the red shifted absorption peak to 400 nm [12]. After addition of Pd NFs/C<sub>60</sub>-NH<sub>2</sub>, the reaction was initiated. The time-dependent UV-vis absorption spectra were recorded to monitor the process of this reaction. The absorption peak at 400 nm decreased successively (Fig. 2B). At the same time, a new absorption peak at around 306 nm appeared by originated from 4-AP, indicating that 4-NP was reduced to 4-AP. It could be observed that its intensity diminished at the later stage of the reaction. As shown in Fig. 2C, according to the linear relationship of  $\ln(C_t/C_0)$  with  $t$ , which agrees with first-order reaction kinetics. The rate constant of the reactions can be estimated for the Pd NFs/C<sub>60</sub>-NH<sub>2</sub> catalysts. It is determined to be 1.805 min<sup>-1</sup>. The conversion rate in the presence of Pd NFs/C<sub>60</sub>-NH<sub>2</sub> was much fast, which could be attributed to (i) the big surface area of nanoflowers, (ii) three-dimensional Pd

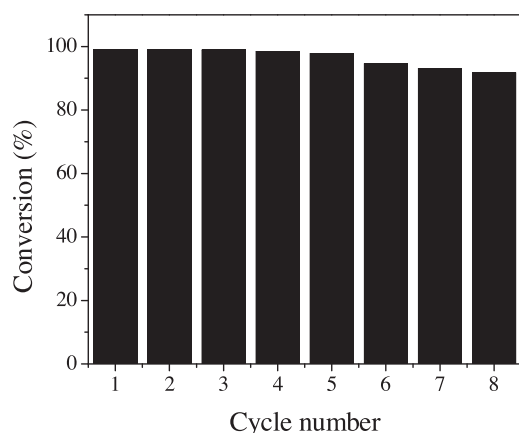


**Fig. 3.** recyclability measurement of Pd NFs/ C<sub>60</sub>-NH<sub>2</sub> during eight successive cycles.

nanostructure and (iii) the synergistic effect between the Pd nanoflower and the C<sub>60</sub>-NH<sub>2</sub> support.

The presence of C<sub>60</sub>-NH<sub>2</sub> can promote to form Pd nanoflower shape and enhance the adsorption of reactant molecules onto the catalytic sites of the Pd nanoparticles through the  $\pi$ - $\pi$  stacking and electrostatic interaction. Moreover, the structure of Pd NFs/ C<sub>60</sub>-NH<sub>2</sub> has no change after the catalytic reaction, which also indicates that the attachment between Pd NFs and C<sub>60</sub>-NH<sub>2</sub> is sufficiently strong. Herein the catalytic activity of the Pd catalyst was also estimated by turnover frequency (TOF). As shown in Table 1, the Pd NFs/C<sub>60</sub>-NH<sub>2</sub> gives a remarkable TOF of 12.35 min<sup>-1</sup> at room temperature. Compared to other similar composites containing Pd-based catalysts [13–17], Pd NFs/C<sub>60</sub>-NH<sub>2</sub> also shows higher catalytic activity for the reaction of reducing 4-NP, suggesting that the self-assembled Pd nanoflowers on C<sub>60</sub>-NH<sub>2</sub>

support is an efficient approach for the preparation of high-performance metal nanocatalysts. For practical applications, the reusability of the catalyst has been studied. As shown in Fig. 3, the conversion of 4-NP could keep over 91% after eight cycles, which exhibits excellent recyclability of the Pd NFs/C<sub>60</sub>-NH<sub>2</sub> catalyst.

In summary, the novel catalyst was prepared by self-assembled palladium nanoflowers supported on amino-functionalized fullerene (C<sub>60</sub>-NH<sub>2</sub>). The Pd nanocomposite exhibited high catalytic activity and stability toward 4-nitrophenol, which will significantly promote catalytic performance due to their ideal morphology.

### Acknowledgment

This work was financially supported by the Natural Science Foundation of Shanxi Province, China (No. 201801D121042).

### References

- [1] X.K. Kong, Z.Y. Sun, M. Chen, C.L. Chen, Q.W. Chen, *Energy Environ. Sci.* 6 (2013) 3260–3266.
- [2] H. Zhang, Q.Q. Ji, L.D. Lai, G. Yao, B. Lai, *Chin. Chem. Lett.* 30 (2019) 1129–1132.
- [3] S. Kubendhiran, R. Sakthivel, S.M. Chen, B. Maharani, T.W. Chen, *Anal. Chem.* 90 (2018) 6283–6291.
- [4] Y. Wang, Q.C. Li, P. Zhang, et al., *J. Colloid Interf. Sci.* 539 (2019) 161–167.
- [5] L.L. Hu, F. Peng, D.H. Xia, et al., *ACS Sustain. Chem. Eng.* 6 (2018) 17391–17401.
- [6] B.Z. Zheng, X.X. Liu, D. Xiao, et al., *Inorg. Chem. Front.* 4 (2017) 1268–1272.
- [7] B. Lang, H.K. Yu, *Chin. Chem. Lett.* 28 (2017) 417–421.
- [8] K. Gu, X.T. Pan, W.W. Wang, et al., *Small* 14 (2018) 1801812.
- [9] L. Zhang, K. Doyle-Davis, X.L. Sun, *Energy Environ. Sci.* 12 (2019) 492–517.
- [10] H.J. Wang, L.J. Bai, Y.Q. Chai, R. Yuan, *Small* 10 (2014) 1857–1865.
- [11] Z.P. Li, M.N. Ruan, L.H.W. Li, et al., *J. Electroanal. Chem.* 805 (2017) 47–52.
- [12] P. Veerakumar, R. Madhu, S.M. Chen, et al., *J. Mater. Chem. A* 2 (2014) 16015–16022.
- [13] J. Liu, J.F. Hao, C.C. Hu, et al., *J. Phys. Chem. C* 122 (2018) 2696–2703.
- [14] Y. Tang, R. Huang, C. Liu, et al., *Anal. Methods* 5 (2013) 5508–5514.
- [15] S. Choi, M. Oh, *Angew. Chem. Int. Ed.* 58 (2019) 866–871.
- [16] C. Zhang, S. Govindaraju, K. Giribabu, Y.S. Huh, K. Yun, *Sens. Actuators B: Chem.* 252 (2017) 616–623.
- [17] D.R. Kumar, M.L. Baynosa, J.J. Shim, *Electrochim. Acta* 246 (2017) 1131–1140.